Experimental investigation of cohesive soil erosion caused by translating submerged inclined water jets

Alhaddad, S.M.S.; Snyder, A.L.; Bult, S.V.; Keetels, G.H.

DOI
10.1016/j.apor.2025.104486

Publication date
2025

Document Version
Final published version

Published in
Applied Ocean Research

Applied Ocean Research 157 (2025) 104486

Contents lists available at ScienceDirect

Applied Ocean Research

journal homepage: www.elsevier.com/locate/apor

Research paper

Experimental investigation of cohesive soil erosion caused by translating submerged inclined water jets

Said Alhaddad *, Andrew Snyder, Sterre V. Bult, Geert Keetels

Section of Offshore and Dredging Engineering, Faculty of Mechanical Engineering, Delft University of Technology, Delft, The Netherlands

ARTICLE INFO

Keywords:
Impinging jet
Inclined jet
Translating jet
Cohesive sediment
Dredging

ABSTRACT

Very limited research has been carried out to investigate sediment erosion caused by subaqueous inclined water jets, despite the fact that such water jets are used in subsea engineering (e.g., dredging, trenching, and deep sea mining). Therefore, we conducted a set of novel small-scale experiments to primarily study the effect of jetting inclination on cohesive sediment erosion. The experimental results reveal that vertical jetting results in the largest cavity depth (or 'erosion depth'), but not in the largest cavity size (sediment production). The erosion depth increases with the jetting angle reaching its maximum at 90° and then begins to decrease with further increase in the jetting angle. The results also indicate that the cavity width (or 'erosion width') is not necessarily correlated with the impingement region but is instead associated with the erosion-effective jet width—the width of the jet where flow velocities are high enough to penetrate the bed. Analysis of the cavity size showed that the largest sediment production was achieved at a 65° jetting angle among the tested jetting angles (25 °, 45 °, 65 °, 90 °, 115 °, 135 °, and 155 °). The erosion depth was found to be highly proportional to the impingement force exerted by the flow on the clay.

1. Introduction

Soil erosion caused by submerged water jets plays a critical role in various applications, such as water injection dredging, the discharge of Trailer Suction Hopper Dredgers, jet trenching, and the collection of polymetallic nodules in deep-sea mining. These applications typically utilize water jets to fluidize sediment, which must be closely monitored to estimate production rates and predict environmental impacts. Although recent research has increasingly focused on inclined water jets, particularly in the context of deep-sea mining (Alhaddad and Helmons, 2023; Liu et al., 2023; Alhaddad et al., 2024), the majority of studies have traditionally concentrated on vertical jets. However, inclined jetting is frequently encountered due to equipment design constraints or specific operational conditions. This operational parameter significantly influences sediment erosion patterns (Hou et al., 2016). In addition, research on cohesive soils has generally been less extensive compared to non-cohesive soils. Given that many jetting applications frequently or predominantly encounter cohesive soils, a thorough understanding of erosion in cohesive soils by a submerged inclined water jet is crucial.

In non-cohesive sediments, maximum penetration depth for stationary water jets was found to depend on multiple jet parameters, including jet velocity, nozzle diameter, and stand-off distance (Aderibigbe and Rajaratnam, 1996). When considering a translating water jet, the ratio between the jet velocity and translating speed additionally governs the penetration depth (Yeh et al., 2009). A laboratory study by Aderibigbe and Rajaratnam (1996) on the erosion of loose sand beds indicated that the penetration depth is inversely related to the median grain diameter and material density. However, Weegenaar et al. (2015) demonstrated that finer sand requires a higher specific energy to fluidize, implying a smaller penetration depth for finer sediment. This can be attributed to the importance of sand permeability at high flow velocities (van Rhee, 2010), as the jet velocities employed by Weegenaar et al. (2015) were significantly higher than those by Aderibigbe and Rajaratnam (1996) and Yeh et al. (2009).

Cohesive soils have a low permeability and high skeleton compressibility. While surface erosion is the dominant mechanism for non-cohesive sediments, the low permeability and cohesive forces prevent this in cohesive sediments. Rather, shear surfaces are developed, with the undrained shear strength as the key sediment characteristic for erosion (Machin et al., 2001). Because of this difference, it has been found difficult to predict scour by impinging jets in cohesive soils using experiments in both non-cohesive and cohesive soils (Mazurek and Hossain, 2007). The literature on erosion of cohesive soils by

* Corresponding author.
E-mail addresses: S.M.S.Alhaddad@tudelft.nl (S. Alhaddad), alsnyder514@gmail.com (A. Snyder), S.V.Bult@tudelft.nl (S.V. Bult), G.H.Keetels@tudelft.nl (G. Keetels).

https://doi.org/10.1016/j.apor.2025.104486
Received 1 August 2024; Received in revised form 28 January 2025; Accepted 20 February 2025

stationary water jets is relatively abundant (Mazurek et al., 2001; Dong et al., 2020; Hou et al., 2016; Feng et al., 2024; Mazurek and Hossain, 2007; Liu et al., 2023), and standard jet erosion tests were developed (Wardinski et al., 2018). Mazurek et al. (2001) showed that the scour hole dimensions depend on the jet velocity, stand-off distance, and the critical shear stress of the soil. Additionally, they observed predominantly mass erosion for scour hole formation. Besides showing the influence of the jet velocity, stand-off distance and critical shear stress, Dong et al. (2020) found that nozzle diameter and scouring duration affect the scour hole dimensions. This reinstates the findings of Moore and Masch (1962) on the importance of time on erosion depth. Scouring time will be especially important for translating jets, with the contact time being limited. Yet, the number of studies on translating submerged jets in cohesive soils is limited. An experimental study on jetting in stiff clay showed that penetration depth is inversely related with the translating velocity (Zhang et al., 2016). From this study, it could also be concluded that the main mechanism causing jet trenching was the boundary layer shear stress. This is in line with Machin and Allan (2011). They noted that for translating velocities exceeding 0.1 to 0.5 m/s, a "quasi-instantaneous" erosion depth occurs, which correlates with the threshold bearing pressure theory. A modelling study by Wang et al. (2021) confirmed the failure process of high-pressure jets in cohesive soils at high translating velocities being a discontinuous process with a given periodicity, with their results clearly showing the shear and pressure evolution over time. In related research on Coandă-effect-based collection, featuring a curved jet, it was shown that there exists a logarithmic relationship between erosion depth and the impinging force (Alhaddad et al., 2024).

To the best of our knowledge, the only study investigating the effect of the angle of inclination on the erosion depth in cohesive soils was performed by Hou et al. (2016). The study by Liu et al. (2023) considered a double-row jet collector at a jetting angle of 45°, but did not vary the angle of inclination. Hou et al. (2016), by combining a theoretical framework and experimental data, showed that the erosion depth increases with increasing angle of inclination in the range of 40–90°. The trend was more prominent for the lower angles of inclination, meaning that for smaller angles the increase in erosion depth was found to be larger. However, to date, no study has examined the effect of the angle of inclination of a submerged translating water jet on the erosion of cohesive soil, and this is the focus of our paper.

The objective of this study is to examine erosion of cohesive soils due to a submerged translating inclined water jet. To this end, we conducted novel small-scale laboratory experiments in a flume where a carriage with half a nozzle drove over clay blocks. The clay had an undrained shear strength of ~30 kPa. We examined how the key jet parameters, consisting of the angle of inclination, translating velocity, nozzle diameter, and stand-off distance, affect the erosion of the cohesive soil. To quantify that, we considered the erosion depth and erosion width. In addition, we show the relation between the flow vertical impingement force and erosion depth.

2. Flow development theory

In the flow field of an impinging jet, previous studies have identified three specific regions: the free-jet region, impingement region and wall-jet region (see Fig. 1). The free-jet region is characterized by the formation of a shear layer between the jet and the ambient water. The transfer of mass and momentum accelerates the ambient water, whereas the jet velocity is increasingly hindered with distance from the jet exit. The potential core is the region where the velocity is equal to jet exit velocity, which reaches up to 4–6D. The bulk mean velocity is often assumed to be uniform at the jet exit, but the exit velocity fits the empirical 1/7 power law of fully developed pipe flow more accurately (Fairweather and Hargrave, 2002; Wang et al., 2017):

$$\frac{V}{V_{max}} = \left(1 - \frac{2r}{D}\right)^{1/7}, \tag{1}$$

where V is the velocity at a certain point in the jet axis, V_{max} is the maximum velocity at the jet centreline, r is the point in the jet axis and D is the diameter of the jet. When the geometrical centre of the jet is penetrated by the turbulence, the flow is fully developed. The velocity decreases rapidly in the impingement zone and the significant pressure gradients cause the flow to deflect. For vertical jets, the point of stagnation pressure and zero velocity will intersect with the geometrical centre at the bed (Beltaos, 1976). The height of the impingement zone is approximately half of the jet diameter at the top of this zone. In the wall-jet region, the deflected flow is parallel to the bed and the static pressure is equal to the ambient pressure.

While the flow field of a vertical circular impinging jet can be assumed to be axisymmetric, this is not the case for an inclined jet. The distribution of the flow in forward and backward direction largely depends on the angle of inclination. It was found that for a stationary impinging jet, for $\theta \leq 26°$ the flow will be entirely in forward direction (Mishra et al., 2020). Previous research on inclined jets assumes the presence of a stagnation point, even for relatively small angles, which distance to the geometrical centre increases with decreasing angle of inclination (Beltaos, 1976; Wang et al., 2017). For a decreasing angle of inclination and constant stand-off distance, the distance from the jet exit to the bed increases. This will cause the velocity decay to be higher compared to vertical jets, leading to smaller velocities near the bed.

Moving the water jet at a certain translating speed will affect the flow deflection. Particle image velocimetry (PIV) measurements conducted by Amin (2022) for a vertical impinging jet showed that the ratio between the translating velocity and jet velocity, R, determines the amount of forward and backward flow. At a point between 0.28 and 0.4 (the particular value has yet to be established) the flow will be fully backward directed (Fig. 2). It remains to be investigated how the angle of inclination affects the deflection of the flow.

3. Laboratory experiments

The experiments involve securing blocks of cohesive soil inside a flume along a transparent wall. A water jet, adjusted to various heights and angles, makes passes along the length of a flume wall. Elevation measurements are taken before and after each pass to determine the erosion depth, which is calculated as the difference between the pre-test and post-test measurements. In addition, the erosion width (the width of the resulting cavity) is measured after each test. In this section, we describe the experimental setup, instrumentation, test procedure and characterization of clay, respectively.

3.1. Experimental setup

The experiments are carried out in a rectangular glass tank measuring 3 m in length, 0.2 m in width, and 0.4 m in depth. To facilitate creating the target jet, several half-circular nozzles were designed and fabricated from resin. For measurements and visualization, the nozzles were positioned as close as possible to the front wall of the flume (see Fig. 3). To allow the jet to traverse, it was fastened on a mobile carriage that can automatically run along bespoke railways at the top of the water flume with a constant, but controllable speed. Each run is video-recorded to examine the erosion of the sediment. A centrifugal pump with a discharge range of 125–400 l/min was used for testing.

A focal point of the experiments are the clay blocks, which are positioned in the middle of the flume, with one side securely pressed against the front wall; wooden spacer was placed to press the clay against the glass (see Fig. 4). To mitigate any softening of the clay, careful measures are implemented to ensure that the clay block remains submerged for the briefest possible duration.

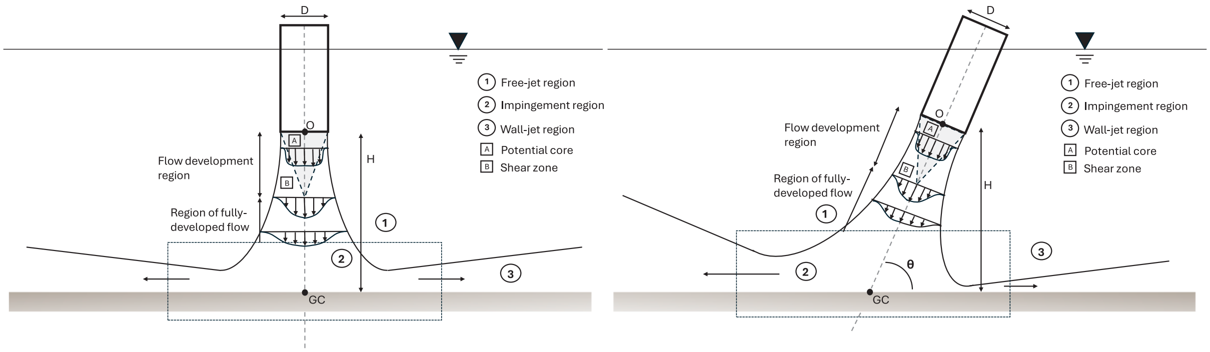

Fig. 1. Flow development of a vertical (left) and inclined (right) circular stationary submerged jet impinging on a flat bed (adapted from Wang et al. (2017) and Nobel (2013)). O indicates the origin of the jet axis, whereas GC indicates the geometrical centre of the jet. θ illustrates the inclination of the jet relative to the bed.

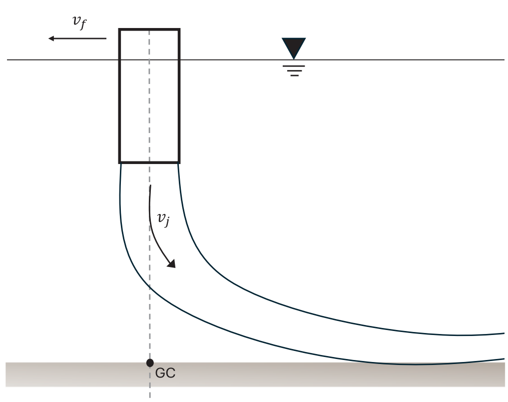

Fig. 2. Flow development of a vertical translating impinging water jet moving to the left (adapted from Amin (2022)). GC indicates the geometrical centre of the jet, v_f the translating velocity and v_j the jet velocity.

Table 1
A summary of the experiments conducted within this study. Z_c and W_c denote the erosion depth and erosion width, respectively.

Test #	D [mm]	SOD [cm]	v_f [m/s]	v_j [m/s]	θ [°]	Z_c [mm]	W_c [mm]
1	17	5	0.40	11.9	25	9	23
2	17	5	0.40	11.7	45	14	34
3	17	5	0.40	12.1	65	17	37
4	17	5	0.40	11.9	90	20	15
5	17	5	0.40	12.1	115	18	24
6	17	5	0.40	11.0	135	16	22
7	17	5	0.40	11.9	155	9	23
8	17	5	0.17	12.7	65	19	45
9	17	5	0.28	12.7	65	18	47
10	17	5	0.55	12.9	65	14	40
11	12	5	0.40	12.2	135	10	25
12	20	5	0.40	12.2	135	21	38
13	12	5	0.40	11.6	45	11	30
14	20	5	0.40	12.0	45	14	40
15	20	10	0.40	12.4	45	8	34

3.2. Instrumentation

The experimental setup was equipped with an electromagnetic flow meter, which was connected to the jet hose to monitor the flow rate through it and to assure that the target jet velocity was achieved for the experiment. An optical sensor was used to measure the erosion depth at several locations at the sediment bed. Besides, a high-speed camera was used to collect visual data from the experiment. This camera was placed in front of the flume and its view was set on the clay blocks.

3.3. Test procedure and data acquisition

To test the vertical jet scenario, the nozzle is positioned at a certain distance above the original clay surface. The vertical distance between the jet exit and the surface of the clay block is referred to as the 'stand-off distance' (SOD). It is important to note that the jetting distance (s) is equal to the SOD in a vertical jet scenario. However, this is not the case when an inclined jet is used. Since the jet has a jetting angle θ, which is the angle from the soil surface to the nozzle, the jetting distance can be calculated using trigonometry as $s = SOD/\sin\theta$ (see Fig. 5).

Every test was conducted 2–3 times following the next sequence of steps:

- Two clay blocks are placed in the middle of the flume and secured to the flume wall by pressing them against the glass until they no longer move or separate from the flume wall.
- The desired nozzle diameter (12 mm, 17 mm, or 20 mm) is connected to the water jet, the correct angle (25°, 45°, 65°, 90°, 115°, 135°, or 155°) is confirmed, and the correct stand-off distance (5 or 10 cm) is set.
- Ten points spaced by a distance of 4 cm along the two clay blocks are marked, and the starting height of the clay at each of these points is measured using an optical sensor.
- The flume is filled to about 25 cm from the bottom of the flume (or just until the water jet is completely submerged) to prevent the flume from overflowing once the test begins.
- The water jet is started at the target flow rate, and the test is commenced. Since the flow rate was adjusted manually using a valve, it was not possible to set the water jet exactly at the target flow velocity. However, the flow rate and jet velocity corresponding to each test were recorded.
- The jet is run at a forward velocity of ≈0.4 m/s for the majority of the test (a variation of forward velocities is also tested as a variable in later tests). There is a sensor at the end of the flume to ensure a quick stop of the carriage.
- The final height of the clay is measured at the ten points that were previously marked. The difference between the starting heights and end heights will be used as the erosion depth achieved by the nozzles. Measurements of the cavity width at the ten points were also collected after each test.

Table 1 summarizes the experiments and measurements conducted within this study. It is worth noting that each experiment was conducted three times in most cases and the erosion depths and widths documented in the table are the average values. The rationale behind the design of the test matrix was to include a wide range of jetting angles (Tests 1–7) to enable a thorough investigation of the effect of jetting angle on cavity dimensions. Following these tests, other key parameters were systematically varied for inclined water jets to study their effects. For instance, the effect of jet forward velocity was

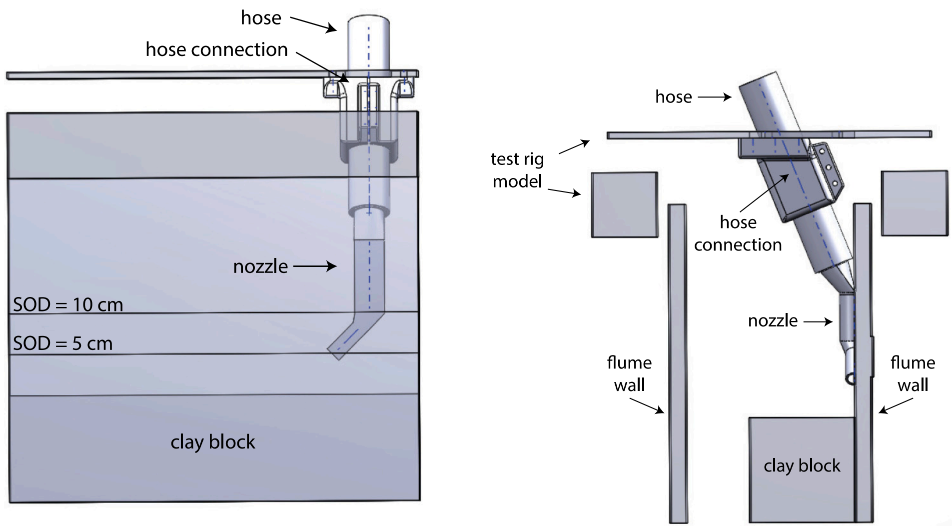

Fig. 3. The 45° nozzle placed against the glass wall of the flume and located 5 or 10 cm above the clay block depending on the test being conducted.

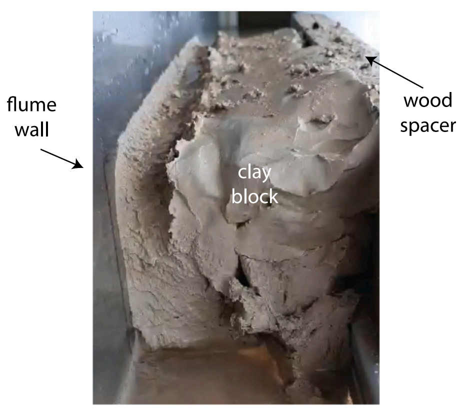

Fig. 4. Post-test photo demonstrating how the clay is secured between the flume wall and the wood spacer.

examined by varying it (Tests 3 and 8–10) while keeping the other parameters constant, including maintaining the jetting angle at 65°.

3.4. Characterization of clay

Clay blocks measuring 13 × 12.5 × 30 cm were ordered from the company "Keramikos" for use in the experiments. Consistent sourcing from a single supplier ensures uniformity in the block composition (see Fig. 6 left) and the undrained shear strength of the clay samples. The blocks are made of a light terracotta clay with a firing range between 1000 °C and 1250 °C, resulting in durable, hard-fired pieces. This clay (d_{50} = 1.3 μm) contains 0% chamotte, meaning it has no added grog or sand, giving it a fine and smooth texture. The grain size distribution of the clay is depicted in the right panel of Fig. 6. The clay preparation process begins with deflocculation. Afterward, dried kaolin powder (see Table 2) is gradually added to the water while stirring slowly. For every 100 kg of kaolin powder, 25 l of water are required; we measured the water content and found it to be 25%. The Consolidated Undrained Triaxial Compression Test determined the undrained shear strength to be 30 kPa.

4. Experimental results

In the following, we will analyse the relationship between sediment erosion and key jet parameters.

Table 2
Chemical analysis of the dried kaolin powder (Kaolin, 2021).

Component	Typical [%]	Warranty [%]
SiO_2	47.5	
AL_2O_3	36.9	>36.0
Fe_2O_3	0.90	<0.95
TiO_2	0.23	<0.30
MgO	0.35	
CaO	0.23	
K_2O	0.90	<1.20
Na_2O	0.05	
LOI	12.8	

4.1. Jetting angle

The jetting angle θ is defined as the angle between the jet axis and the sediment bed. To explore its effect on the cavity, we conducted experiments with jetting angles ranging from 25° to 155°. Fig. 7 shows the resulting cavities after three tests. The erosion depths were measured for experimental runs of different jetting angles (see Fig. 8 left). It can clearly be seen that, when $\theta < 90°$, a higher θ results in a larger erosion depth, a trend similar to the observations of Hou et al. (2016) for stationary jets. In contrast, when $\theta > 90°$, a higher θ results in a smaller erosion depth. Besides, it is observed that the erosion depth is maximal, when $\theta = 90°$. Interestingly, supplementary jetting angles render approximately the same erosion depths.

We also measured the cavity width (or 'erosion width') for the tests of different jetting angles (see Fig. 8 right). It can manifestly be seen that the erosion width is minimal when $\theta = 90°$. This is attributed to the fact that $\theta = 90°$ renders the smallest jetting distance, s, and by extension the smallest impingement region (when s is larger more water will be entrained to the jet). Although supplementary angles (e.g., 45 and 135°) render the same s, they resulted in different erosion widths. This is because the water jets were moving, meaning that they deflected differently, consequently resulting in different impingement regions. It should also be noted that erosion width does not always correlate with the impingement region, as will be discussed in Section 4.4.

Looking into the erosion depth is insufficient to explore the effect of jetting angle on clay production. Instead, the cavity size should be quantified and studied. To this end, we calculated the cross-sectional area of the cavity, assuming that the cavity takes a rectangular shape (see Fig. 9). The results show that $\theta = 90°$ does not result in the largest clay production, though it renders the largest erosion depth. Jetting angles smaller than 90° result in larger erosion areas than

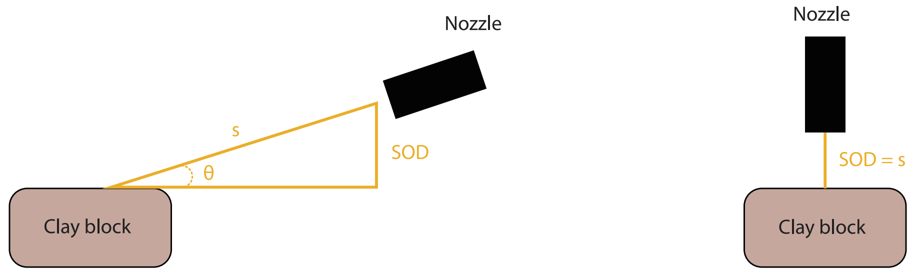

Fig. 5. Illustration of the difference between stand-off distance, SOD, and the jetting distance, s.

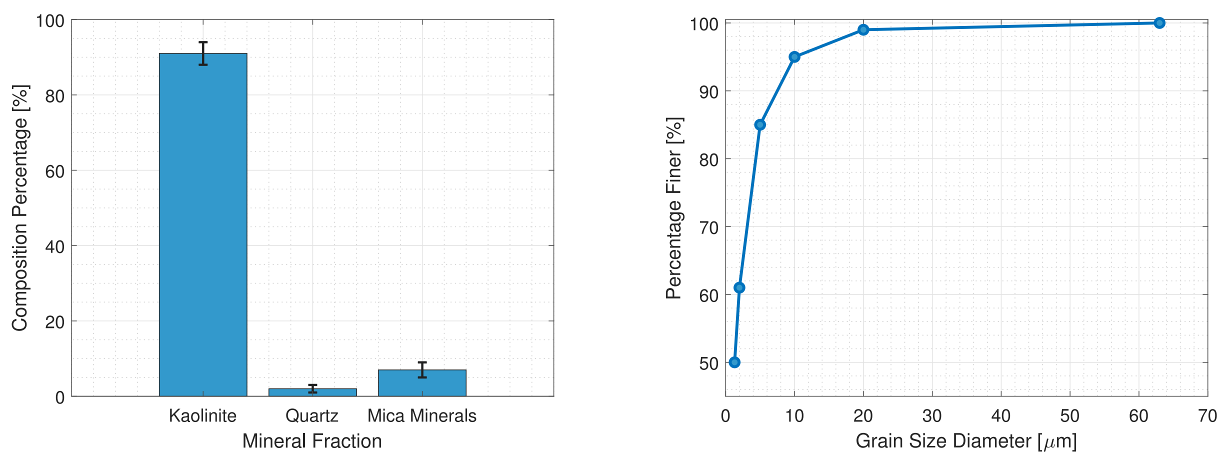

Fig. 6. Mineral composition of the clay (left). Cumulative grain size distribution for the clay used in the experiments (right); particles larger than 63 μm < 0.1% (Kaolin, 2021).

Fig. 7. Cavity resulting from Test 7 (top): D = 17 mm, θ = 155°, SOD = 5 cm, v_f = 0.4 m/s and v_j = 11.9 m/s. Cavity resulting from Test 6 (middle): D = 17 mm, θ = 135°, SOD = 5 cm, v_f = 0.4 m/s and v_j = 11 m/s. Cavity resulting from Test 5 (bottom): D = 17 mm, θ = 115°, SOD = 5 cm, v_f = 0.4 m/s and v_j = 12.1 m/s.

jetting angles larger than 90°, mainly because of larger erosion widths. Among the tested jetting angles (25°–155°), θ = 65° resulted in the greatest clay production. However, the optimal jetting angle for clay production could be somewhere between 65° and 90°, a range that was not tested in our study. It is noteworthy that the suspended-sediment environmental pressure (Alhaddad and Elerian, 2024), along with production, should be taken into consideration when selecting the optimal jetting operational conditions.

4.2. Jet forward velocity

This section will focus on the effect of the forward translating velocity, v_f, of an inclined water jet on the erosion process of cohesive soil. The range of velocities tested is 0.17 to 0.55 m/s as depicted in Fig. 10. Unsurprisingly, the experimental results demonstrate that a larger v_f leads to a smaller erosion depth. This correlation is expected, mainly because a larger v_f means that the clay is exposed to the water

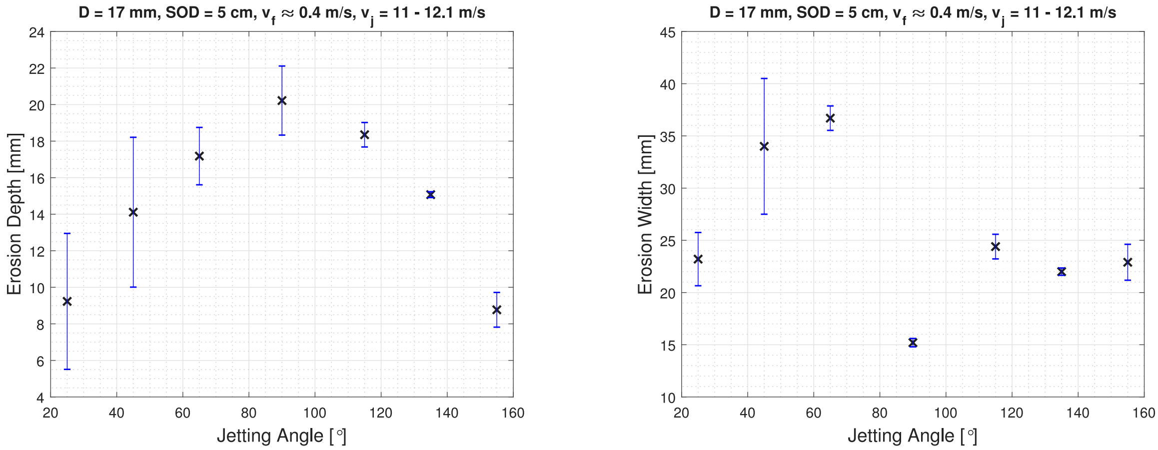

Fig. 8. Effect of jetting angle on the erosion depth (**left**) and erosion width (**right**).

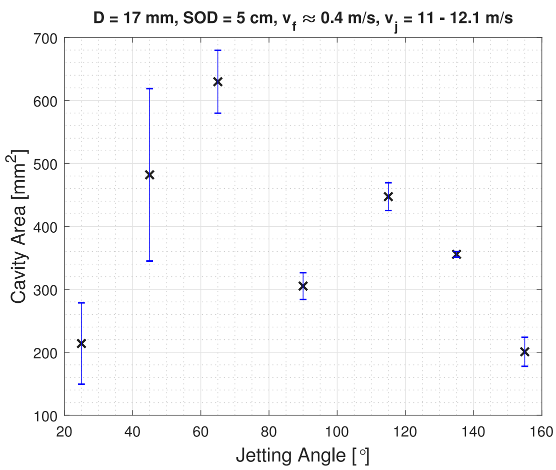

Fig. 9. The average effect of jetting angle on the cavity area [mm^2]. The erosion area is defined as the erosion depth, Z_c, multiplied by the erosion width, W_c. The error bars show the standard deviation of the production area. This was determined by computing the joint distribution.

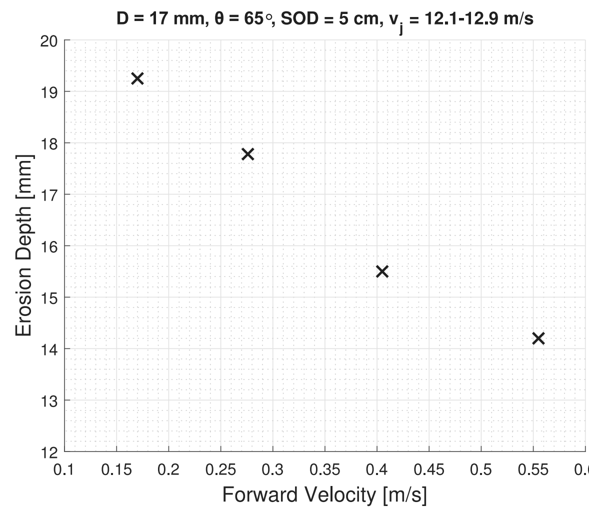

Fig. 10. Effect of jet forward velocity on the erosion depth.

jet for a shorter duration, consequently eroding less sediment. It should also be noted that a change in forward velocity results in a change in jet deflection (Amin, 2022), and consequently, in the flow velocities just above the clay bed.

4.3. Nozzle diameter

This section will focus on the impact of the nozzle diameter of an inclined water jet on the erosion process of cohesive soil. Considering jetting angles of 45° and 135° (see Fig. 11), a conspicuous correlation between the nozzle diameter and cavity dimensions is found as depicted in Fig. 12. Erosion depth displays an incremental pattern with increasing nozzle diameter. The employment of the smallest nozzle diameter (12 mm) yielded the least erosion. This outcome is expected since the entrainment of the surrounding water affects the jets of smaller nozzle areas more than those of larger nozzle areas. A 20 mm nozzle has a larger area and therefore the jet velocity just above the clay is larger, allowing for a greater erosion depth.

A similar tendency is observable in the right panel of Fig. 12 for the erosion width. The reason for this is that as the nozzle diameter expands, a larger water jet is brought into contact with the soil (i.e., larger impingement region), resulting in a correspondingly increased erosion width.

It is noteworthy to mention again that we used half-circular nozzles placed directly against the tank wall. This configuration suppresses flow on the wall side entirely, leaving no room for water entrainment on that side. The jet velocity at the wall is zero due to the no-slip condition, and wall friction leads to some dissipation of momentum near the wall. In contrast, the mean flow of a full-circular free jet is symmetric, although the turbulent structures responsible for entrainment are not. This difference could result in a greater amount of entrainment in the full-circular nozzle case, where these structures can develop freely without the limitation of the wall. Thus, we hypothesize that for the full-circular nozzle, the cavity depth would be smaller, and the cavity width would be larger compared to the half-circular nozzle case.

4.4. Stand-off distance

A clear trend is observed between the stand-off distance and cavity dimensions (Fig. 13). A smaller stand-off distance results in a larger erosion depth, because the mean jet velocity right above the clay is larger. Although a larger SOD means more water entrainment and by extension larger impingement region, SOD = 10 cm resulted in a bit smaller erosion width than SOD = 5 cm. This means that larger impingement region does not necessarily result in a larger erosion width. Instead, the erosion width is correlated with the erosion-effective jet width (the jet width that has flow velocities large enough to penetrate the bed).

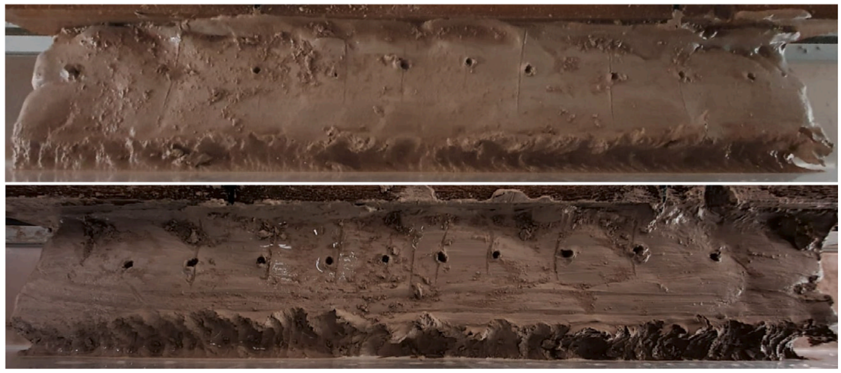

Fig. 11. Cavity resulting from Test 11 (top): D = 12 mm, $\theta = 135°$, SOD = 5 cm, v_f = 0.4 m/s and v_j = 12.2 m/s. Cavity resulting from Test 12 (bottom): D = 20 mm, $\theta = 135°$, SOD = 5 cm, v_f = 0.4 m/s and v_j = 12.2 m/s.

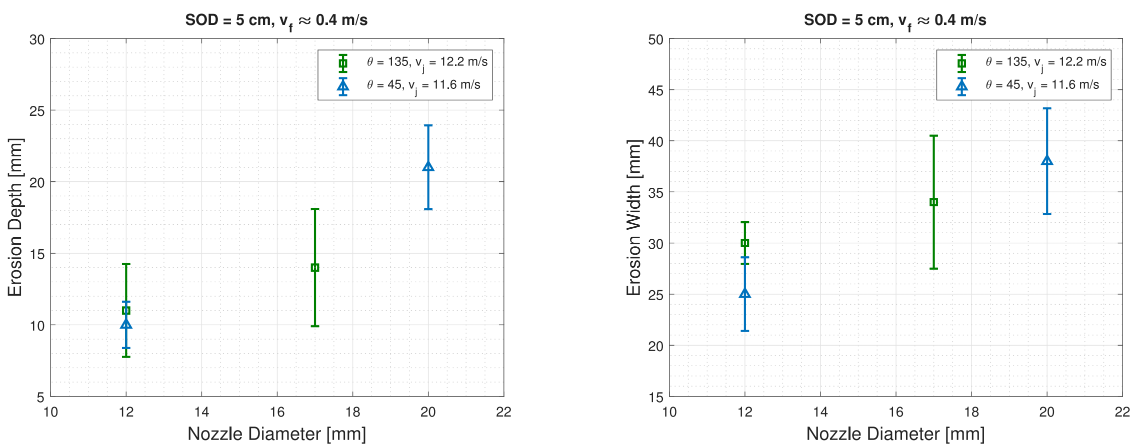

Fig. 12. Effects of nozzle diameter on the erosion depth (**left**) and erosion width (**right**).

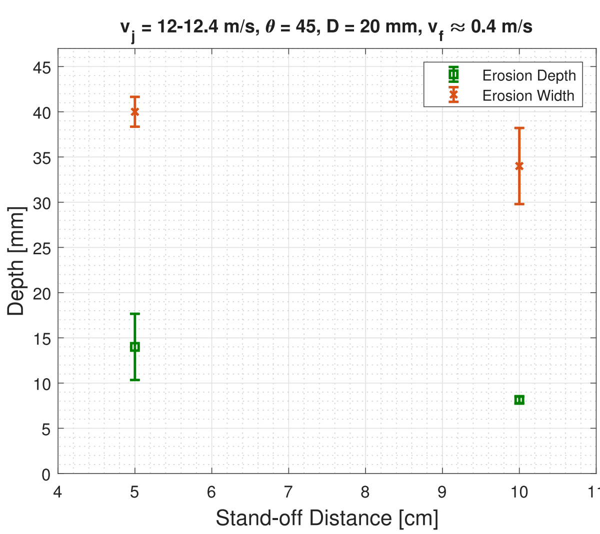

Fig. 13. Effect of stand-off distance on the cavity dimensions (erosion depth and width).

4.5. Flow impingement force

Clay erosion is a complicated process that involves the detachment and transport of fine particles with strong inter-particle bonds. Alhaddad et al. (2024) revealed that the erosion depth resulting from inclined water jets created by a hydraulic collector is proportional to the flow impingement force on a clay bed. Here, we investigate whether such a correlation also holds for our experiments. Calculating the total impingement force would require knowing the flow velocities at the wall-jet region, which were not retrieved within this study. For simplicity, we calculate the vertical impingement force F_y, which reads:

$$F_y = \rho A v_j^2 \sin\theta \tag{2}$$

where ρ is water density and A is the nozzle area.

In our analysis, we consider all experimental runs in which v_f = 0.4 m/s, as these represent the vast majority of the tests performed. Fig. 14 illustrates a strong correlation between the vertical impingement force and the measured erosion depth. The data indicates that erosion depth increases with higher vertical impingement forces. Such a correlation provides a convenient practical tool once a certain erosion depth should be met in practice.

4.6. Comparison with other experimental data

The existing body of literature does not include data on cohesive soil erosion caused by translating submerged inclined water jets. Nonetheless, very limited data on the erosion of cohesive soil by translating submerged vertical water jets is available. For instance, Nobel (2013) conducted laboratory experiments and found that the normalized erosion depth Z_c/D is positively correlated with the normalized jet pressure p_j/s_u, where p_j is the jet pressure and s_u is the clay undrained shear strength. In this subsection, we revisit his experimental data and compare it with our own, as shown in Fig. 15. Since we only conducted one test with $\theta = 90°$, we use our data for $\theta = 65°$. The jetting distances (s) in all experiments shown in the figure (0.67D–3.25D) are smaller than the lengths of the corresponding potential cores (Lee and

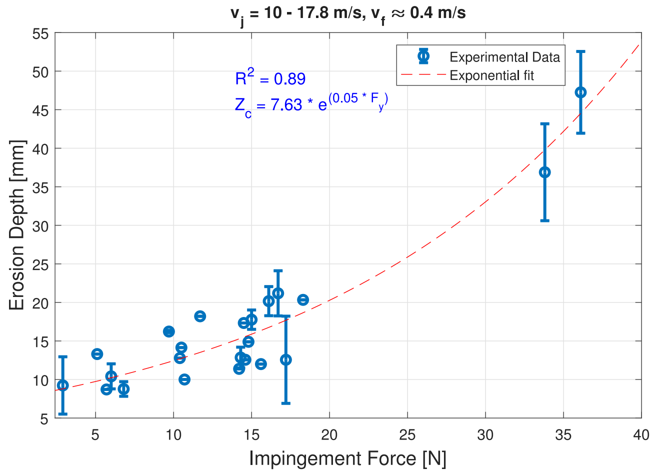

Fig. 14. Relationship between the vertical impingement force and the measured erosion depth.

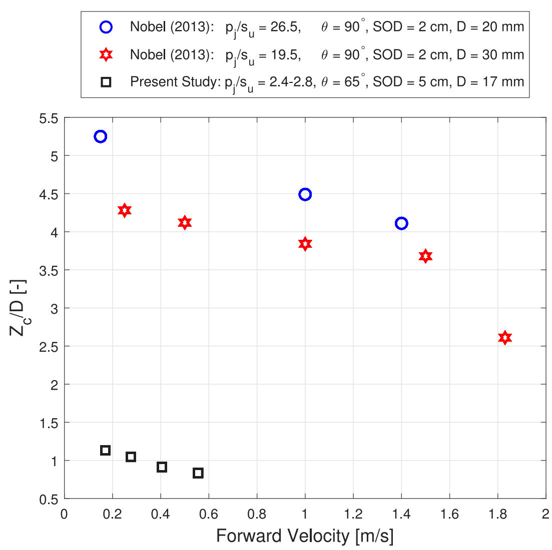

Fig. 15. Relationship between jet forward velocity and normalized erosion depth Z_c/D.

Chu, 2012; Hashiehbaf et al., 2015), implying that the effect of s on the erosion depths is limited. Indeed, Fig. 15 confirms that a higher p_j/s_u results in a larger Z_c/D. Additionally, the experimental measurements of Nobel (2013) demonstrate that a larger forward velocity leads to a smaller erosion depth, as shown by our data and discussed in Section 4.2.

5. Discussion and conclusions

We carried out a set of novel small-scale experiments to explore clay erosion caused by translating submerged inclined water jets. In these experiments, several jet operational conditions were tested, demonstrating the effect of a handful of critical parameters on sediment erosion.

The following jetting angles were tested: 25°, 45°, 65°, 90°, 115°, 135°, and 155°. The experimental results unravel that the erosion depth increases with the jetting angle, peaking at 90°, and then decreases as the angle increases further. Interestingly, supplementary jetting angles rendered approximately the same erosion depths but different erosion widths. Although vertical jetting rendered the maximal erosion depth, it resulted in the minimal erosion width. Since clay production (the amount of material excavated) is a crucial factor for some practical applications like dredging engineering, we analysed the impact of jetting inclination on the cavity size. The maximum clay production occurred at a jetting angle of 65° among the tested angles. However, based on the data trend, the optimal jetting angle for clay production could be somewhere between 65° and 90°, a range that was not tested in our study.

It is also found that the jet forward velocity is inversely related to the erosion depth, since the clay is exposed to the water jet for a shorter duration when the jet translates quicker and vice versa. Another playing factor is that a change in forward velocity results in a change in jet deflection, and consequently, in the flow velocities just above the clay bed. In the future, we plan to conduct experiments to study in detail how the flow field of a translating inclined water jet is affected by the operational parameters, including jet forward velocity.

Our study also indicates that the erosion width does not necessarily correlate with the impingement region but rather with the erosion-effective jet width — the width of the jet where flow velocities are sufficiently high to penetrate the sediment bed. Careful analysis of the experimental results demonstrated that the erosion depth is strongly proportional to the vertical impinging force exerted by the flow on the clay. This observation aligns with the finding of Alhaddad et al. (2024) and implies that the force exerted by the flow on the bed is the key parameter to be optimized to either maximize or minimize the erosion depth, depending on the application.

CRediT authorship contribution statement

Said Alhaddad: Writing – review & editing, Writing – original draft, Visualization, Supervision, Project administration, Methodology, Investigation, Formal analysis, Data curation, Conceptualization. **Andrew Snyder:** Visualization, Methodology, Investigation, Formal analysis, Data curation, Conceptualization. **Sterre V. Bult:** Writing – original draft, Visualization. **Geert Keetels:** Writing – review & editing, Supervision.

Declaration of competing interest

The authors declare that they have no known competing financial interests or personal relationships that could have appeared to influence the work reported in this paper.

References

Aderibigbe, O.O., Rajaratnam, N., 1996. Erosion of loose beds by submerged circular impinging vertical turbulent jets. J. Hydraul. Res. 34 (1), 19–33. http://dx.doi.org/10.1080/00221689609498762.

Alhaddad, S., Elerian, M., 2024. Mitigating suspended-sediment environmental pressure in subsea engineering through colliding turbidity currents. Res. Eng. 101916.

Alhaddad, S., Helmons, R., 2023. Sediment erosion generated by a Coandă-effect-based polymetallic-nodule collector. J. Mar. Sci. Eng. 11 (2), 349.

Alhaddad, S., Suleman, M., Kirichek, A., Chassagne, C., 2024. Experimental investigation of cohesive soil erosion and suspension caused by a Coandă-effect-based polymetallic-nodule collector. Res. Eng. 22, 102231. http://dx.doi.org/10.1016/j.rineng.2024.102231.

Amin, M.R., 2022. Erosion and Air Entrainment by Stationary and Translating Circular Jets (Ph.D. thesis). University of Alberta.

Beltaos, S., 1976. Oblique impingement of circular turbulent jets. J. Hydraul. Res. 14, 17–36. http://dx.doi.org/10.1080/00221687609499685.

Dong, C., Yu, G., Zhang, H., Zhang, M., 2020. Scouring by submerged water jet vertically impinging on a cohesive bed. Ocean Eng. 196, http://dx.doi.org/10.1016/j.oceaneng.2019.106781.

Fairweather, M., Hargrave, G.K., 2002. Experimental investigation of an axisymmetric, impinging turbulent jet. 1. Velocity field. Exp. Fluids 33, 464–471. http://dx.doi.org/10.1007/s00348-002-0479-7.

Feng, C., Kong, L., Wang, Y., Lu, J., 2024. Experimental study on scouring by submerged pulsed waterjet vertically impinging on cohesive bed. Ocean Eng. 298, 117308. http://dx.doi.org/10.1016/j.oceaneng.2024.117308.

Hashiehbaf, A., Baramade, A., Agrawal, A., Romano, G.P., 2015. Experimental investigation on an axisymmetric turbulent jet impinging on a concave surface. Int. J. Heat Fluid Flow 53, 167–182.

Hou, J., Zhang, L., Gong, Y., Ning, D., Zhang, Z., 2016. Theoretical and experimental study of scour depth by submerged water jet. Adv. Mech. Eng. 8, 1–9. http://dx.doi.org/10.1177/1687814016682392.

Kaolin, S., 2021. Kaolin zettlitz ia. Online; https://www.keramikos.nl/website/database/uploads/Datasheets/Kaolien.pdf. (Accessed 10 October 2024).

Lee, J.H.-w., Chu, V., 2012. Turbulent Jets and Plumes: A Lagrangian Approach. Springer Science & Business Media.

Liu, X., Chen, X., Wei, J., Jin, S., Gao, X., Sun, G., Yan, J., Lu, Q., 2023. Study on sediment erosion generated by a deep-sea polymetallic-nodule collector based on double-row jet. Ocean Eng. 285, 115220. http://dx.doi.org/10.1016/j.oceaneng.2023.115220.

Machin, J.B., Allan, P.A., 2011. State-of-the-art jet trenching analysis in stiff clays. In: Frontiers in Offshore Geotechnics II. Taylor & Francis Group, pp. 871–876.

Machin, J.B., Messina, F.D., Mangal, J.K., Girard, J., 2001. Recent research on stiff clay jetting. In: OTC 13139.

Mazurek, K.A., Hossain, T., 2007. Scour by jets in cohesionless and cohesive soils. Can. J. Civ. Eng. 34 (6), 744–751. http://dx.doi.org/10.1139/l07-005.

Mazurek, K.A., Rajaratnam, N., Sego, D.C., 2001. Scour of cohesive soil by submerged circular turbulent impinging jets. J. Hydraul. Eng. 127, 598–606. http://dx.doi.org/10.1061/(ASCE)0733-9429(2001)127:7(598).

Mishra, A., Yadav, H., Djenidi, L., Agrawal, A., 2020. Experimental study of fow characteristics of an oblique impinging jet. Exp. Fluids 61, 90. http://dx.doi.org/10.1007/s00348-020-2923-y.

Moore, W.L., Masch, F.D., 1962. Experiments on the scour resistance of cohesive sediments. J. Geophys. Res. 67 (4), 1437–1446. http://dx.doi.org/10.1029/JZ067i004p01437.

Nobel, A., 2013. On the Excavation Process of a Moving Vertical Jet in Cohesive Soil (Ph.D. thesis). Delft University of Technology.

van Rhee, C., 2010. Sediment entrainment at high flow velocity. J. Hydraul. Eng. 136, 572–582. http://dx.doi.org/10.1061/(ASCE)HY.1943-7900.0000214.

Wang, B., van Rhee, C., Nobel, A., Keetels, G.H., 2021. Modeling the hydraulic excavation of cohesive soil by a moving vertical jet. Ocean Eng. 227, 108796. http://dx.doi.org/10.1016/j.oceaneng.2021.108796.

Wang, C., Wang, X., Shi, W., Lu, W., Tan, S.K., Zhou, L., 2017. Experimental investigation on impingement of a submerged circular water jet at varying impinging angles and Reynolds numbers. Exp. Therm. Fluid Sci. 89, 189–198. http://dx.doi.org/10.1016/j.expthermflusci.2017.08.005.

Wardinski, K.M., Guertault, L., Fox, G.A., Castro-Bolinaga, C.F., 2018. Suitability of a linear model for predicting cohesive soil detachment during jet erosion tests. J. Hydrol. Eng. 23 (9), http://dx.doi.org/10.1061/(ASCE)HE.1943-5584.0001690.

Weegenaar, R.A., Keetels, G.H., Winkelman, M.O., van Rhee, C., 2015. Sand erosion with a traversing circular jet. Marit. Eng. 168 (MA2), 76–83. http://dx.doi.org/10.1680/maen.14.00004.

Yeh, P.-H., Chang, K.-A., Henriksen, J., Edge, B., Chang, P., Silver, A., Vargas, A., 2009. Large-scale laboratory experiments on erosion of sand beds by moving circular vertical jets. Ocean Eng. 36, 248–255. http://dx.doi.org/10.1016/j.oceaneng.2008.11.006.

Zhang, S., Zhao, M., Ge, T., Wang, C., 2016. Experimental research on trenching in stiff clay by submerged vertical traveling jets. J. Coast. Res. 32, 365–373. http://dx.doi.org/10.2112/JCOASTRES-D-14-00038.1.